Indoor Radiated-Mode Leaky Feeder Propagation at 2.0 GHz

Y. P. Zhang

***Abstract*—This paper presents the results of narrow-band and wide-band propagation measurements carried out at 2.0 GHz in an indoor environment using a radiated-mode leaky feeder as the transmitting antenna. The narrow-band measurements were devised to measure attenuation of radio signals and the wide-band techniques to measure multipath impulse responses and their associated root mean square (rms) delay spread. Analysis of the narrow-band data files shows that the received signal levels in the direction along the feeder generally decay exponentially due to the feeder-specific attenuation. The received signal levels in the direction radial to the feeder decrease slowly, and the distance–power law exponent is found to be smaller than one. The slow and fast variations of the received signal levels are also examined. The results reveal that the slow variations basically follow the log-normal distribution, while the fast variations fit the Rayleigh distribution in the direction parallel to the feeder and the Rician distribution in the direction radial to the feeder, respectively. Analysis of the wide-band data files reveals that the maximum value of the rms delay spread is 60.6 ns and the rms delay spread values are less than 42 ns 50% of the time. One therefore can conclude that the indoor channel excited by the radiated-mode leaky feeder has a broad coherent bandwidth and can support the data rate up to 3.3 Mb/s without equalization.**

***Index Terms*—Indoor propagation, leaky feeder, wireless communications.**

I. Introduction

LEAKY feeders have been used for many years to provide mobile and personal communications services in tunnels. Recently, they have found applications in indoor wireless personal communications systems [1]–[3]. There have been several measurements of leaky feeder propagation inside buildings. Bye reported the measurements in a typical office building at 200 and 900 MHz and demonstrated that by properly routing the leaky feeder along the corridor or around the corners specific, perhaps otherwise impossible, coverage requirements could be met [4]. Motley and Keenan studied a 900-MHz leaky feeder laid in the corridor of a building and found that the spatial variations in the received signal level were well represented by a Rayleigh distribution [5]. Davies *et al.*compared the radio coverage at 1700 MHz using a dipole and a leaky feeder as the transmitting antennas. Their preliminary results showed that the propagation loss was inversely proportional to the longitudinal distance for the leaky feeder and the penetration loss was on the same order of magnitude for both cases [6]. All these measurements were designed to determine the propagation loss for the coverage problem of leaky feeder systems inside buildings; few attempts were made to measure the time dispersion of leaky feeder propagation for wide-band systems. In fact, detailed knowledge of the time dispersion is essential because unsatisfactory performance in wide-band systems can also be caused by intersymbol interference due to delay spread, and this limits the data rate even within the intended coverage area.

Thus, in order to fully characterize indoor leaky feeder radio propagation channels, we conducted a series of narrow-band and wide-band propagation measurements in a large building. The narrow-band measurements were devised to measure attenuation of radio signals and the wide-band techniques to measure multipath impulse responses and their associated root mean square (rms) delay spread. A radiated-mode leaky feeder was employed in our measurements. It operated at 2.0 GHz functioning as the transmitting antenna to simulate leaky feeders used as the base-station antennas in real systems. The frequency selected at 2.0 GHz is that of interest for International Mobile Telecommunications 2000. We report the measurements in this paper. A description of the experimental site, systems, and techniques required to perform the proposed measurements is given in Section II. Both narrow-band and wide-band measurement results are presented and discussed in Section III. Finally, Section IV summarizes the conclusions.

II. Measurements

The measurements are described as follows.

A. Measurement Systems

Both our narrow-band and wide-band measurement systems were set up using off-the-shelf equipment. The narrow-band system consisted of three modules: an HP 44233B signal source used as the transmitter, an HP 8563E spectrum analyzer utilized as the receiver, and a personal computer employed as the data collector. The narrow-band system was calibrated at 2.0 GHz with 110-dB dynamic range. The wide-band system was an HP 8753D network analyzer: Port 1 of the network analyzer used as the transmitter; Port 2 utilized as the receiver; and the built-in disk driver employed as the data collector. The wide-band system was operated at the central frequency of 2.0 GHz with frequency spectrum over the range of 400 MHz, which yields an equivalent resolution of 2.5 ns and a repetition period of 500 ns in the time domain.

The transmitting antenna for both systems was a leaky feeder terminated with a matched load. The leaky feeder had a coaxial design. Its configuration is shown in Fig. 1. As shown, six slots are grouped and arranged in a periodic pattern. Actually, the six slots can be considered as a combined aperture. The separation

Manuscript received May 18, 2000; revised September 8, 2000.

The author is with the School of Electrical and Electronic Engineering, Nanyang Technological University, 639798 Singapore (e-mail: eypzhang@ntu.edu.sg).

Publisher Item Identifier S 0018-9545(01)01227-0.

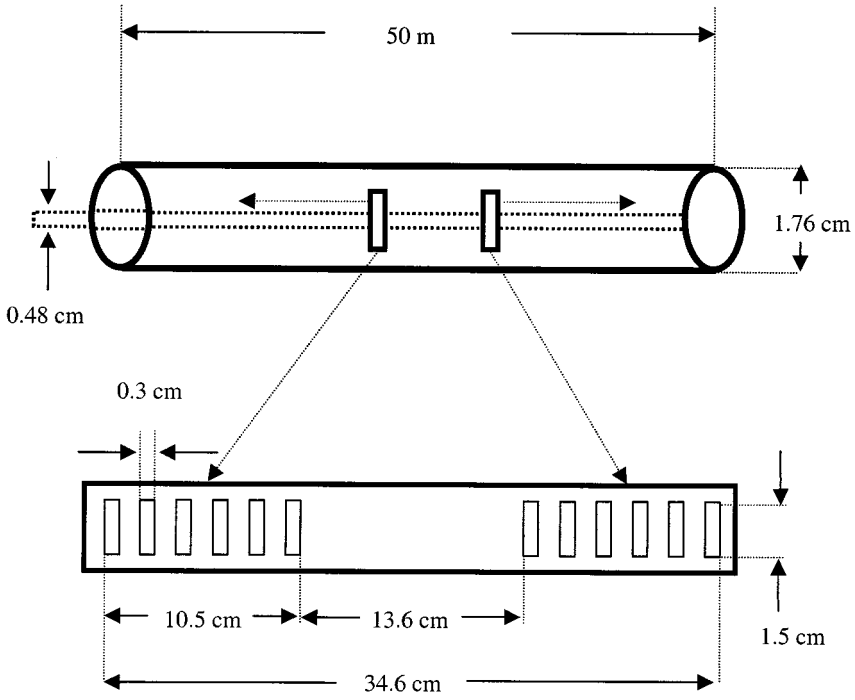

Fig. 1. The configuration of the radiated-mode leaky feeder.

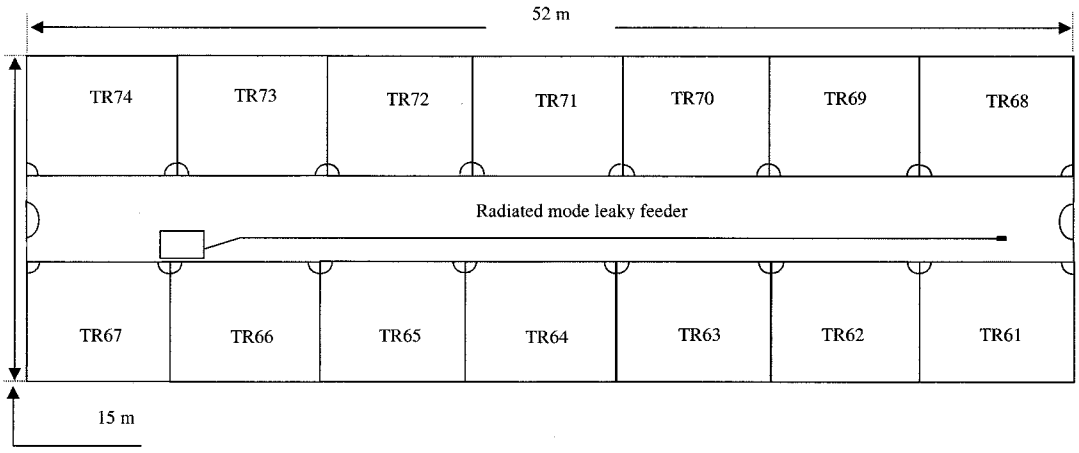

Fig. 2. The layout and dimensions of the measurement site.

between the two adjacent apertures is 13.6 cm. This aperture spacing distance is comparable to the operational wavelength 15 cm. Hence the leaky feeder was a radiated-mode type. This radiated-mode leaky feeder radiated radially.

The receiving antenna was a half-wave dipole for the narrow-band system and a discone for the wide-band system.

B. Measurement Site

The measurements were made on floor B1 of the Academic Complex South Spine of Nanyang Technological University, Singapore. The floor is made of reinforced concrete. The ceiling is 3.83 m high, with a suspended tile false ceiling at 2.83 m. Air-condition trucking and electrical cables run above the false ceiling. The floor is partitioned into rooms with internal brick and external glass walls. These rooms are all interconnected by a single corridor. The layout and dimensions of the floor are sketched in Fig. 2. Room 70 is left empty for reference purposes. Other rooms have chairs and tables all over the surface.

C. Measurement Procedures

The installation of the radiated-mode leaky feeder in the middle of the corridor below the ceiling 0.6 m is also shown in Fig. 2. It is seen that a portion of the leaky feeder is lowered down to connect to the transmitter. We divided our measurement efforts into two distinct categories.

1) *Dynamic narrow-band measurements:* We measured attenuation of radio signals when the receiving antenna at the height of 1.22 m above the floor was being moved at a constant speed together with the receiver and data collector housed on a trolley. Six data points were recorded over a wavelength of 15 cm. This recording rate was sufficient to follow the peaks and nulls of the fading, which

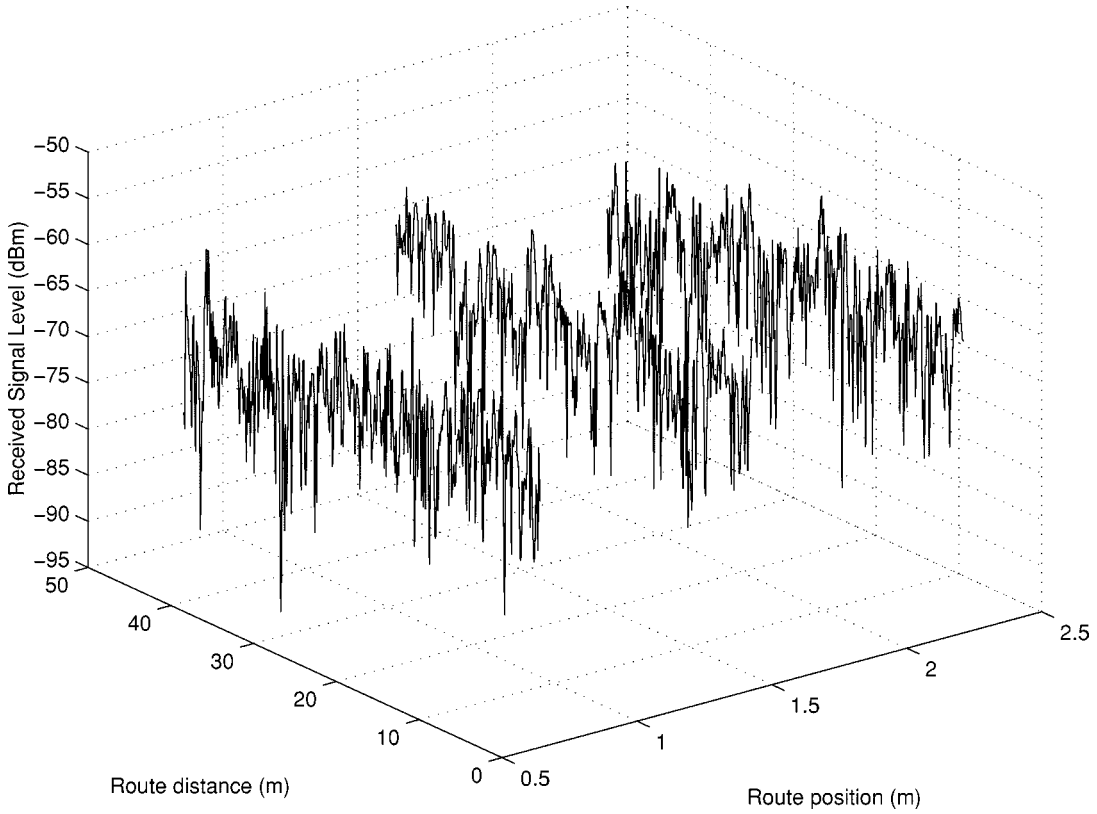

Fig. 3. The received signal levels in the corridor.

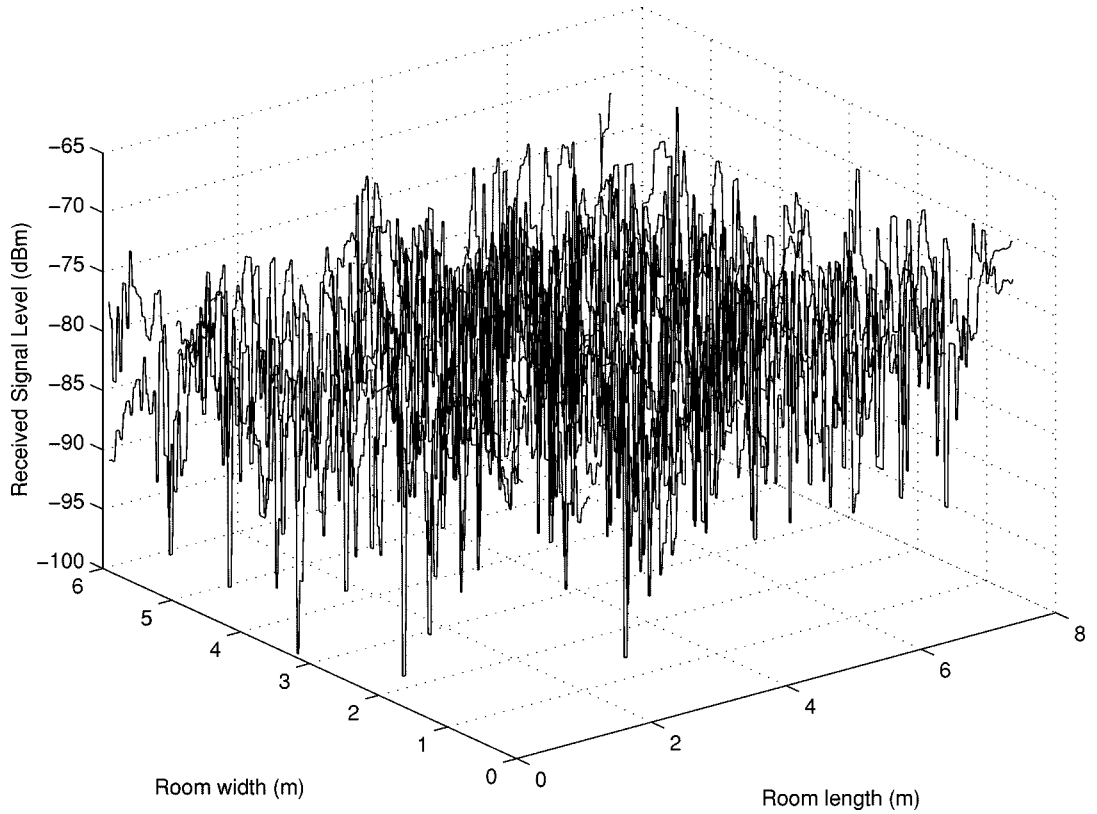

Fig. 4. The received signal levels in the room.

was expected to appear at every wavelength. Measurements were first taken along routes in the corridor and then taken along routes in rooms. Routes in the corridor were all parallel to the axis of the leaky feeder, while of

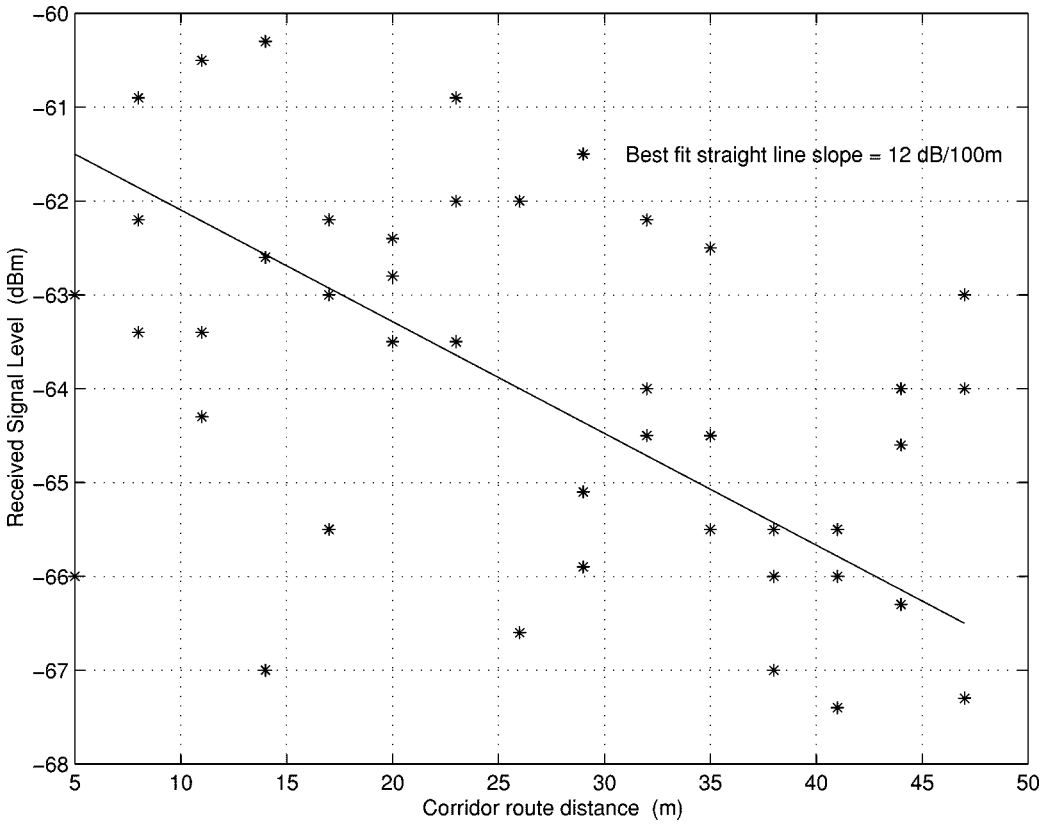

Fig. 5. The local mean signal levels in the corridor.

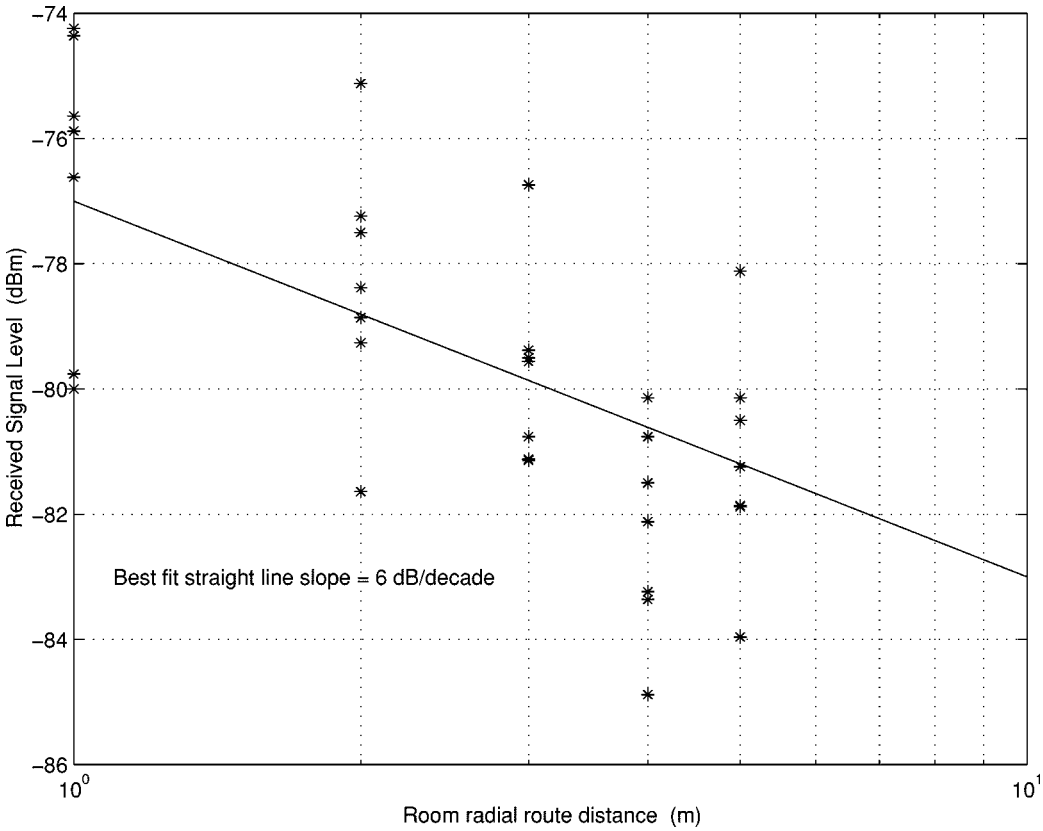

Fig. 6. The local mean signal levels for the room radial routes.

the routes in rooms, some were parallel and others were radial to the axis of the leaky feeder.

2) *Static wide-band measurements:* We measured multipath impulse responses when the receiving antenna was sta-

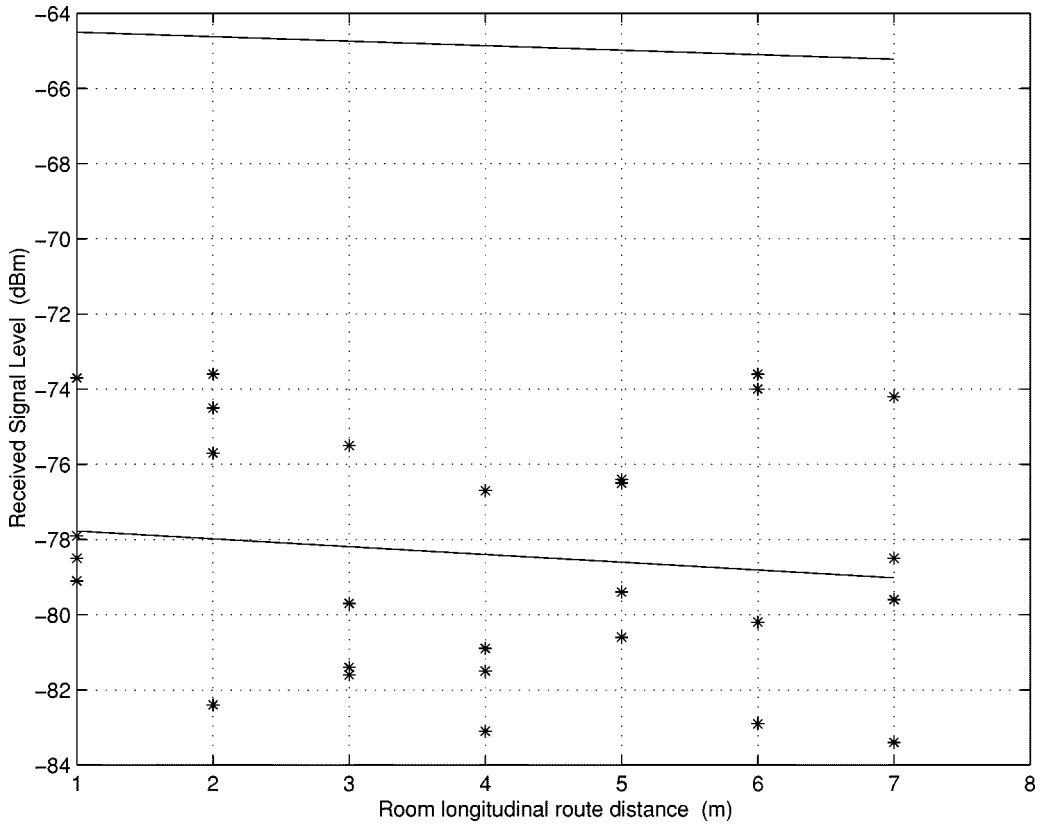

Fig. 7. The local mean signal levels for the room longitudinal routes.

tionary also at the height of 1.22 m above the floor. Measurements were taken on a cluster scale with the cluster having a size of 16 cm^2. The adjacent cluster on a route either parallel or radial to the cable was 1 m apart for most measurements. Four individual impulse responses were obtained for each cluster. Each individual impulse response was measured over several hundred microseconds. They were then averaged at each time delay to calculate an averaged impulse response to simulate a time-invariant condition. This averaged impulse response was used to calculate the rms delay spread for the cluster.

During the measurements, it was observed that the orientation of the receiving antenna strongly influenced the received signal levels. As vertical polarization is widely adopted in wireless personal communications systems, the orientation of both half-wave dipole and discone antennas was vertical.

III. Results and Discussions

Radio propagation from the radiated-mode leaky feeder inside a building can be expressed by an equation similar in form to that for conventional antennas as follows:

$$P_r = P_t - \alpha Z - L_c - L_v - L_b - 10n\log_{10}(D) \qquad (1)$$

where

- P_r received power;
- P_t transmitted power;
- Z distance along the cable to the point nearest the receiver;
- α attenuation per unit length of the cable;
- L_c coupling loss referenced to 1-m radial distance from the cable;
- L_v variability in coupling loss;
- L_b loss factor due to blockage;
- D distance between the cable and the receiver;
- n loss exponent.

The aim of the narrow-band measurements has been to quantify the unknown parameters in this equation.

A. Propagation Loss

Typical plots of the narrow-band received signal levels versus distance are shown in Figs. 3 and 4 for the corridor and the reference room, respectively. It is seen that for both cases, the received signal levels fluctuate over the whole routes. Large fluctuations in the received signal levels are due to the changing phasor sum of signal components arriving at the receiving antenna via different paths. It is also seen that the received signal levels are stronger in the corridor than those in the room. This is because the received signal traveled a shorter radial distance in the corridor, while the received signal not only propagated a longer radial distance but also underwent the wall penetration loss into the room. For the corridor case, it is noted that the received signal levels appear stronger along the middle route than those along the side routes. The route-dependent difference in the received signal levels is mainly attributed to the radiation pattern of the leaky feeder. Since the slots of the leaky feeder were installed facing downwards, this resulted in the occurrence of the downward maximum radiation. Therefore, the received signal levels were observed stronger along the middle route. For

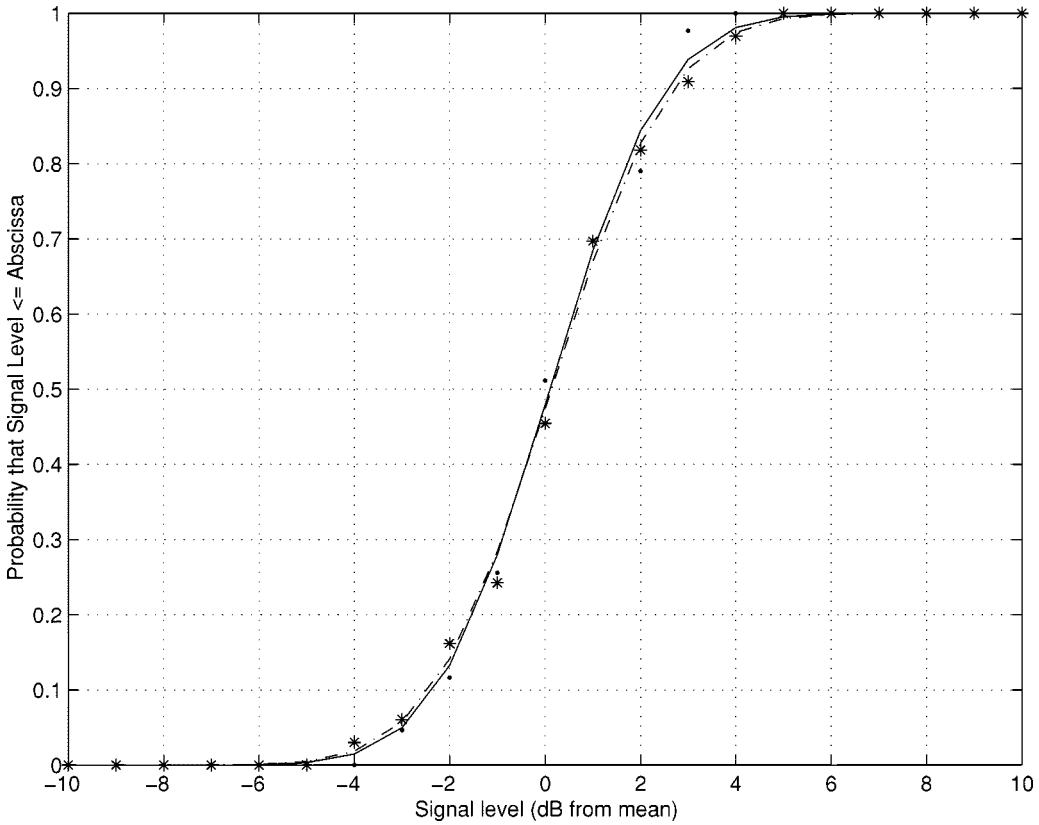

Fig. 8. Cumulative distribution of signal levels of slow variations.

the room case, it is evident that there is a slight decrease in the received signal levels along a route parallel to the axis of the leaky feeder. However, there is a considerable decay in the received signal levels along a route radial to the axis of the leaky feeder.

The analysis of a narrow-band received signal data file first requires obtaining its local mean. The moving average method has been used to estimate the local mean of the received signal in our work [7]. Fig. 5 shows the mean signal levels for the corridor as the leaky feeder plotted against the distance from the nearest point on the leaky feeder back to the transmitter. A straight line that gives the best fit to the mean signal levels is also plotted. The slope of this line 12 dB/100 m represents the attenuation of the signal propagating along the length of the leaky feeder, corresponding to the factor α in (1). In addition, Fig. 5 actually shows the mean signal levels 1.0 m radially away from the leaky feeder. This is because an appropriate amount of 2.5 dB radial propagation loss was removed from the mean signal levels along the side routes since the side routes had a radial distance of 1.44 m, while no correction for radial propagation loss was made to the mean signal levels along the middle route since the middle route just had the radial distance of 1.0 m from the leaky feeder. As a result, Fig. 5 can also be used to estimate the coupling loss L_c in (1) as follows. The input signal level to the leaky feeder was 10 dBm, the mean received signal level—say, at corridor route distance 30 m—is -64.5 dBm, as shown in Fig. 5, and the attenuation of the signal propagating along the leaky feeder of 30 m is 3.6 dB, so the coupling loss L_c is found to be $P_t - P_r - \alpha Z = 10 - (-64.5) - 0.12 \cdot 30 = 70.9$ dB.

Fig. 6 shows the mean signal levels for the room radial routes. In this case, the routes were radial to the axis of the leaky feeder and with the different longitudinal distances with respect to the transmitter, so the mean signal levels have been adjusted to account for different amounts of attenuation along the leaky feeder. They now represent the mean signal levels in the room middle radial route. A straight line that gives the best fit to the mean signal levels is also plotted. The slope of this line represents the attenuation of the signals propagating radially away from the leaky feeder, corresponding to the loss exponent n in (1). This loss exponent $n = 0.6$ was used to determine 2.5-dB correction included in Fig. 5.

Fig. 7 shows the mean signal levels for the room longitudinal routes. In this case, the routes were parallel and with different radial distances to the axis of the leaky feeder, so the mean signal levels have been adjusted to account for different amounts of attenuation from the leaky feeder. They now represent the mean signal levels in the room middle longitudinal route. Two straight lines are also shown in Fig. 7. The lower line gives the best fit to the mean signal levels along the room middle longitudinal route, while the upper line stands for the best fit to the mean signal levels along the room section of the corridor middle route. Note that two lines are parallel, as expected, because the slope of both lines represents the same attenuation factor α in (1). Also note that the mean signal levels in the room middle longitudinal route are 13.2 dB lower than those along the room section of the corridor middle route. The extra path loss due to the longer propagation distance from the leaky feeder and the blockage loss due to the penetration through the wall into the room account for

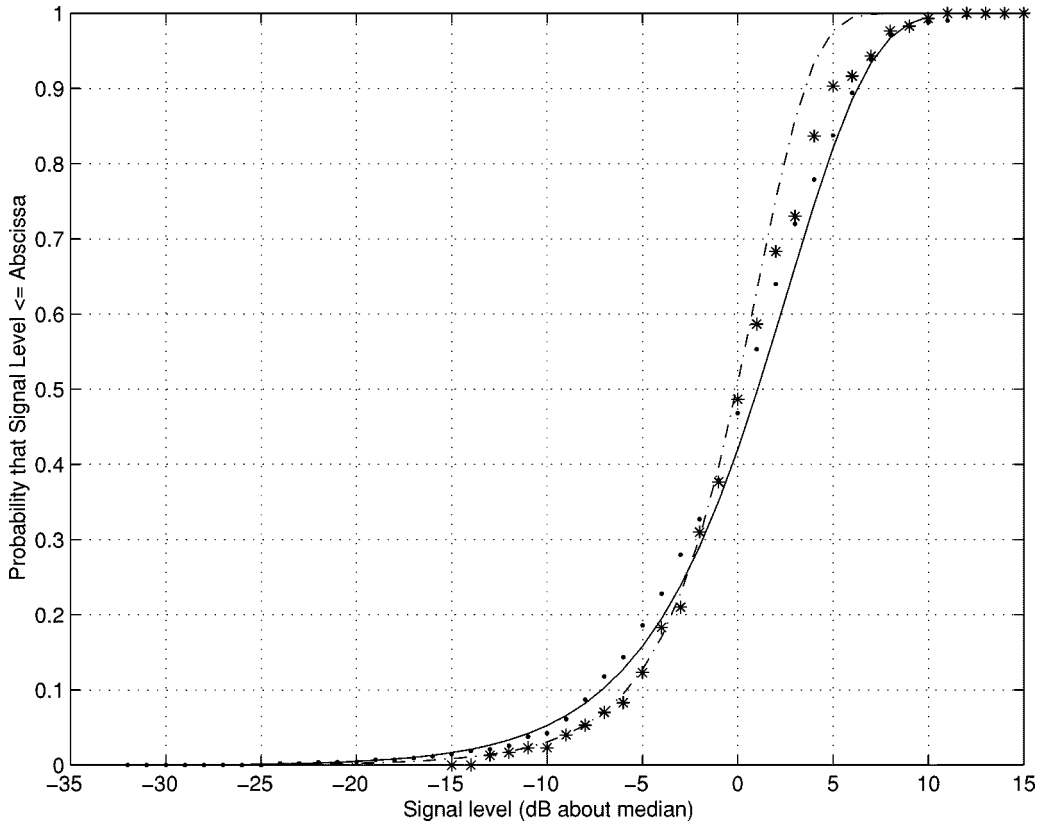

Fig. 9. Cumulative distribution of signal levels of fast variations.

TABLE I
THE PARAMETERS OBTAINED FROM THE MEASUREMENTS

L_c (dB)	L_v (dB)	L_b (dB)	α (dB/100m)	n
70.9	Min. −4.16 Max. 3.4 Mean 0.13 Std. 1.98	9.9 (brick wall)	12	Min. 0.25 Max. 1.025 Mean 0.6 Std 0.28

the lower mean signal levels observed in the room. The extra path loss can be calculated to be $6\log(\Delta d) = 6\log(3.5) = 3.3$ dB. Therefore, the loss factor due to wall blockage L_b can be estimated to be 9.9 dB.

B. Fading Statistics

The fading statistics are examined. The slow fading statistics deals with the remaining variation after removal of the signal-level distance dependence depicted by the best fit line from a mean signal. This is useful in estimating the coverage and cochannel interference. It is found that the slow fading in many other radio propagation environments follows the log-normal distribution. Analysis of our slow variation signals shows that they basically follow the log-normal distribution. This can be seen from Fig. 8. The solid and dot curves represent the log-normal and experimental distributions with the mean of 0.097 dB and standard deviation of 1.88 dB for the corridor case. The dash-dot and asterisk curves stand for the log-normal and experimental distributions with the mean of 0.13 dB and the standard deviation of 1.98 dB for the room case. The fast fading statistics deal with the fast variations of a received signal and are important in determining fluctuation margin in system design. It is known that the fast fading generally fits the Rayleigh distribution. However, the fast fading can be better described with the Rician distribution if there is a main component in the received signal. Analysis of our fast variation signals shows that they fit the Rayleigh distribution in the corridor and the Rician distribution in the room, respectively. This can be seen from Fig. 9. The solid and dot curves express the Rayleigh and experimental distributions with the mean value of -0.1554 dB and the standard deviation of 5.488 dB for the corridor case. The dash-dot and asterisk curves depict the Rician and experimental distributions with a K value of 3.9 dB for the room case. The factor of K defines the ratio of the dominant specular signal component to the random multipath. The formula to calculate it can be

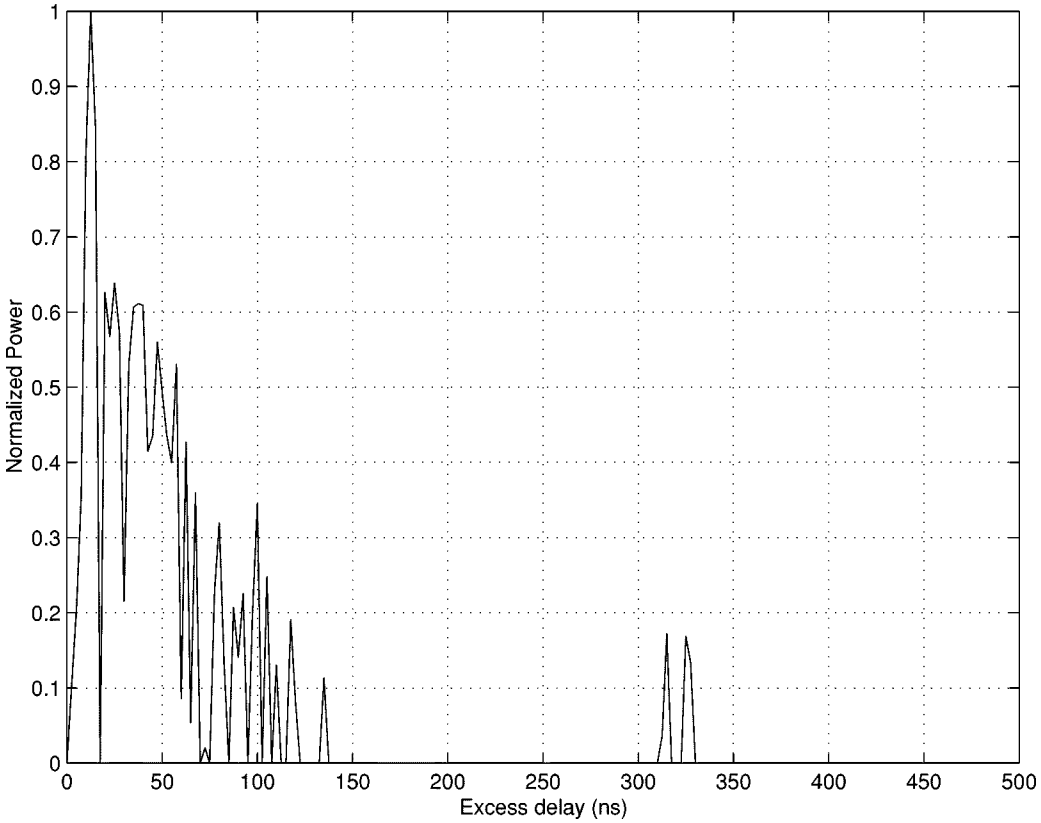

Fig. 10. A typical corridor power-delay profile.

found in [8]. Finally, the quantified parameters for (1) are listed in Table I.

C. Time Dispersion

Future personal communications systems will be wide-band and operate at high data rates. A major problem that degrades the performance of wireless personal communications systems is echoed in transmission caused by multipath propagation. The rms delay spread is a convenient measure of this phenomenon and is extremely useful in determining data rates for unequalized channels. The rms delay spread can be obtained from an impulse response as follows:

$$h_a(\tau) = \int_p h_c(p,\tau)\, dp \tag{2}$$

where the impulse response $h_c(p, \tau)$ is actually a power-delay profile obtained from measurement position p and scaled such that the first wave arrives at $\tau = 0$ in the profile and $h_a(\tau)$ is the space-averaged power-delay profile. The first moment of the power-delay profile with respect to the first arriving wave is given by

$$\overline{\tau} \approx \frac{\sum_k \tau_k h_a(\tau_k)}{\sum_k h_a(\tau_k)}. \tag{3}$$

The rms delay spread is the square root of the second central moment of the power-delay profile and expressed as

$$\tau_{\mathrm{rms}} \approx \left[\frac{\sum_k \tau_k^2 h_a(\tau_k)}{\sum_k h_a(\tau_k)} - (\overline{\tau})^2\right]^{1/2}. \tag{4}$$

Strong echoes with long delays contribute significantly to τ_{rms}. Detailed analysis of τ_{rms} can provide valuable information to designers of wireless personal communications systems.

Prior to analyzing measured impulse responses, it is necessary to set a threshold level. The threshold level is placed at -25 dB down from the largest peak in measured impulse responses in our work.

Fig. 10 shows a typical power-delay profile measured in the corridor. It is seen that there are many echoes above the threshold level. The first group of echoes with excess delay <150 ns is from the leaky feeder and due to the multiple reflections from the floor, walls, and ceiling. The second group of echoes around 320 ns is from the bent section of the leaky feeder at the transmitter and reflected from the corridor door at the termination load. The rms delay spread of this power-delay profile is 57 ns.

Fig. 11 shows a typical power-delay profile measured in the room. Many echoes above the threshold level still can be seen. They all occur before excess delay 100 ns. The echoes around excess delay 320 ns in the previous profile disappear from this profile. This is because they are greatly attenuated by multiple

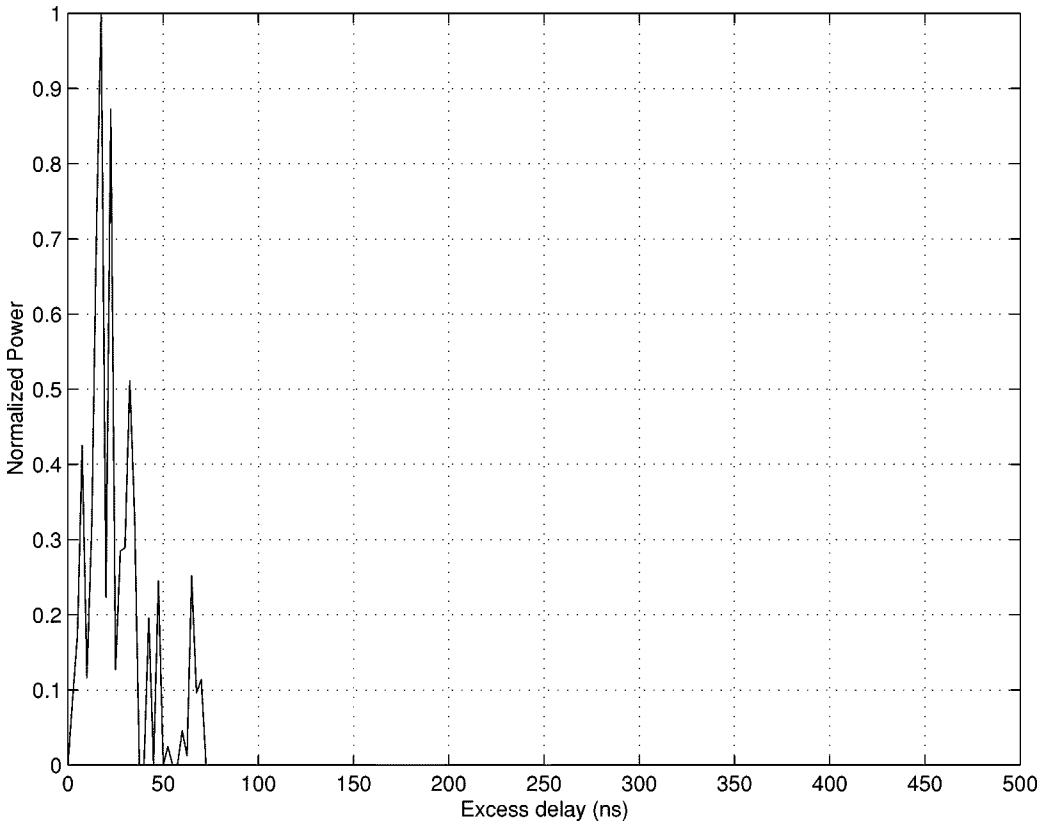

Fig. 11. A typical room power-delay profile.

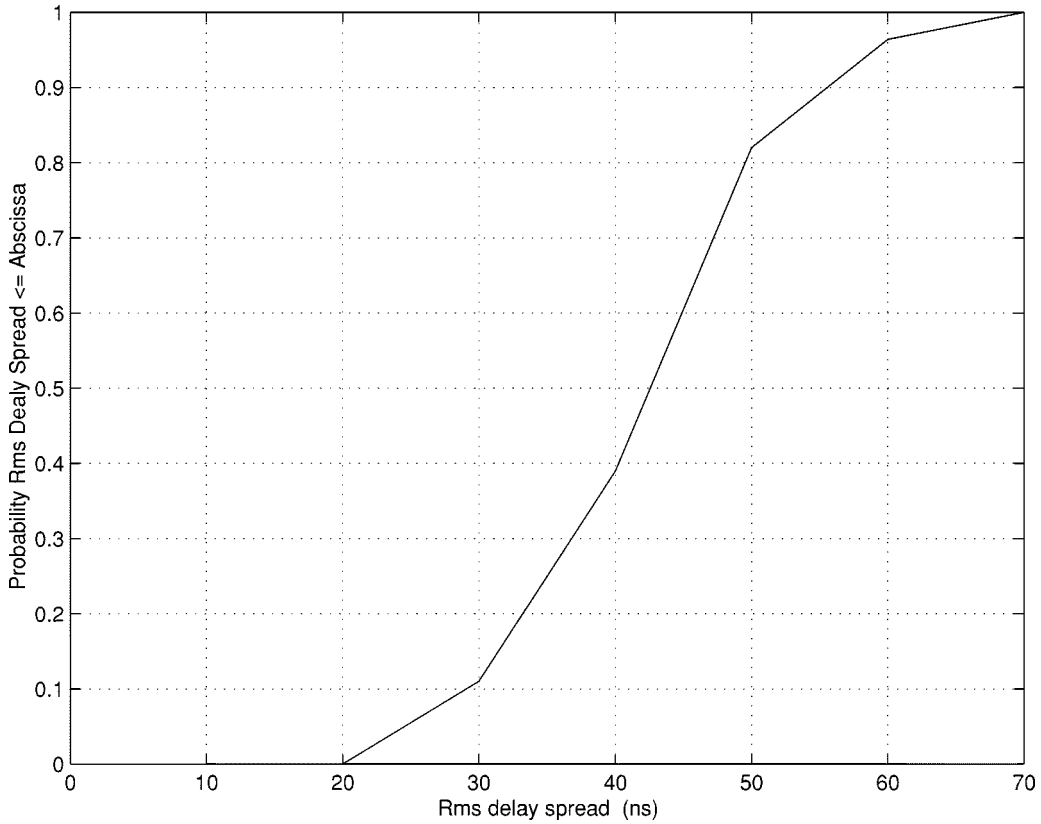

Fig. 12. Cumulative distribution of rms delay spread.

walls in the propagation path. The rms delay spread of this power-delay profile is 16 ns.

Since the rms delay spread values were not normally distributed, it was necessary to employ nonparametric statistical analysis. The statistics of the rms delay spread were compiled. Fig. 12 shows the cumulative distribution. The maximum value of the rms delay spread is 60.6 ns. The rms delay spread values are less than 42 ns 50% of the time. It is well known that performance of wireless personal communications systems operating in multipath environments are very sensitive to rms delay spread values. Simulation studies have shown that without diversity or equalization, the ratio of the rms delay spread to symbol duration in digital transmission must be kept below 0.2 to have a tolerable intersymbol interference [9]. Based on this criterion, the indoor channel excited by the radiated-mode leaky feeder has a broad coherent bandwidth and can support the data rate up to 3.3 Mb/s.

IV. Conclusion

The results of multipath radiated-mode leaky feeder propagation measurements carried out at 2.0 GHz in a building were reported. The narrow-band results showed that the received signal levels in the direction along the leaky feeder generally decayed exponentially. The received signal levels in the direction radial to the cable decreased slowly, and the loss exponent was smaller than one. The slow variations of the received signal levels followed the log-normal distribution in both directions parallel and radial to the leaky feeder. The fast variations of the received signal levels fitted the Rayleigh distribution in the direction parallel to the cable and the Rician distribution in the direction radial to the leaky feeder, respectively.

The wide-band results revealed that the maximum value of the rms delay spread was 60.6 ns and the rms delay spreads were less than 42 ns 50% of the time. Hence the indoor channel excited by the radiated-mode leaky feeder had a broad coherent bandwidth and could support the data rate up to 3.3 Mb/s without equalization.

References

[1] C. Seltzer, "Indoor coverage requirements and solutions," in *Proc. Inst. Elect. Eng. Colloquium Antennas and Propagation for Future Mobile Communications*, 1998, pp. 3/1–3/4.

[2] H. Yanikomeroglu and E. S. Sousa, "CDMA distributed antenna system for indoor wireless communications," in *Conf. Rec. 2nd Int. Conf. Universal Personal Communications*, vol. 2, 1993, pp. 990–994.

[3] A. A. M. Saleh, A. J. Rustako, and R. S. Roman, "Distributed antennas for indoor radio communications," *IEEE Trans. Commun.*, vol. C-35, no. 12, pp. 1245–1251, 1987.

[4] K. J. Bye, "Leaky-feeders for cordless communication in the office," in *Proc. 8th Eur. Conf. Electrotechnics*, 1988, pp. 387–390.

[5] A. J. Motley and J. M. P. Keenan, "Radio coverage in buildings," *Br. Telecom Technol. J.*, vol. 8, no. 1, 1990.

[6] R. Davies, A. Simpson, and J. P. McGeehan, "Preliminary wireless propagation results at 1.7 GHz using a half wave dipole and a leaky feeder as the transmitting antenna," in *Proc. 5th Int. Conf. Radio Receivers and Associated Systems*, 1990, pp. 10–14.

[7] M. Lecours, J. Y. Chouinard, G. Y. Delisle, and J. Roy, "Statistical modeling of the received signal envelope in a mobile radio channel," *IEEE Trans. Veh. Technol.*, vol. 37, no. 4, pp. 204–212, 1988.

[8] T. S. Rappaport and C. D. McGillem, "UHF fading in factories," *IEEE J. Select. Areas Commun.*, vol. 7, no. 1, pp. 40–48, 1989.

[9] J. C. I. Chuang, "The effects of time delay spread on portable radio communications channels with digital modulation," *IEEE J. Select. Areas Commun.*, vol. SAC-5, no. 5, pp. 879–899, 1987.

Y. P. Zhang received the B.E. degree from Taiyuan Polytechnic Institute, Taiyuan University of Technology, Shanxi, China, in 1982, the M.E. degree from Shanxi Mining Institute,Taiyuan University of Technology, in 1987, and the Ph.D. degree from the Chinese University of Hong Kong in 1995, all in electronic engineering.

He was with Shanxi Electronic Industry Bureau (1982–1984), the University of Liverpool, U.K. (1990–1992), and City University of Hong Kong (1996–1997). He taught at Shanxi Mining Institute (1987–1990) and the University of Hong Kong (1997–1998). He has been a full Professor at Taiyuan University of Technology since 1996. Currently, he is a Member of the Faculty of the School of Electrical and Electronic Engineering, Nanyang Technological University, Singapore. His research interests include propagation of radio waves, characterization of radio channels, small and smart antennas, and wireless communications systems. He has authored or coauthored approximately 80 publications.

Prof. Zhang received the Sino-British Technical Collaboration Award in 1990 for his contribution to the advancement of subsurface radio science and technology. He also received an Overseas Research Students Award in 1992 from the Committee of Vice-Chancellors and Principals of the Universities of the United Kingdom and an Excellent Graduate Award in 1995 from the Chinese University of Hong Kong. He received the Best Paper Award from the Second International Symposium on Communication Systems, Networks and Digital Signal Processing, Bournemouth, U.K., in 2000.